A MODEL FOR THE INTERNAL STRUCTURE OF MOLECULAR CLOUD CORES

Dean E. McLaughlin and Ralph E. Pudritz
Department of Physics and Astronomy, McMaster University
Hamilton, Ontario L8S 4M1, Canada
dean@physics.mcmaster.ca, pudritz@physics.mcmaster.ca

ABSTRACT

We generalize the classic Bonnor-Ebert stability analysis of pressure-truncated, self-gravitating gas spheres, to include clouds with arbitrary equations of state. A virial-theorem analysis is also used to incorporate mean magnetic fields into such structures. The results are applied to giant molecular clouds (GMCs), and to individual dense cores, with an eye to accounting for recent observations of the internal velocity-dispersion profiles of the cores in particular. We argue that GMCs and massive cores are at or near their critical mass, and that in such a case the size-linewidth and mass-radius relations between them are only weakly dependent on their internal structures; any gas equation of state leads to essentially the same relations. We briefly consider the possibility that molecular clouds can be described by polytropic pressure-density relations (of either positive or negative index), but show that these are inconsistent with the apparent gravitational virial equilibrium, $2\,\mathcal{U}+\mathcal{W}\approx 0$, of GMCs and of massive cores. This class of models would include clouds whose nonthermal support comes entirely from Alfvén wave pressure. The simplest model consistent with all the salient features of GMCs and cores is a "pure logotrope," in which $P/P_c = 1 + A\,\ln(\rho/\rho_c)$. Detailed comparisons with data are made to estimate the value of A, and an excellent fit to the observed dependence of velocity dispersion on radius in cores is obtained with $A \simeq 0.2$.

To appear in the Astrophysical Journal

1. Introduction

Giant molecular clouds (GMCs; $M \sim 10^5 - 10^6 M_\odot$) in the Galaxy are highly inhomogeneous: they are often filamentary in appearance, consisting of discrete clumps, or cores ($M \lesssim 10^3 M_\odot$), which contain most of the mass of a cloud (including any young stars) and are surrounded by a more diffuse component of predominantly atomic gas (e.g., Williams, Blitz, & Stark 1995). Indeed, GMCs are clumpy on all scales observed, and are possibly even fractal in nature (Falgarone, Phillips, & Walker 1991). Remarkably enough, however, the gross properties of cloud complexes are rather simply interrelated. Total masses, mean densities, and average velocity dispersions vary with sizes (effective radii) roughly as $M \propto R^2$, $\rho_{\rm ave} \propto R^{-1}$, and $\sigma_{\rm ave} \propto R^{1/2}$ (Larson 1981; Sanders, Scoville, & Solomon 1985; Solomon et al. 1987), with uncertainties in the exponents typically of order ± 0.1. The seeming universality of these results demands a physical explanation.

The relationship between size and linewidth (which term we use interchangeably with velocity dispersion) is further interesting because σ is observed to decrease towards smaller radii *inside* GMCs, and within individual dense cores (Larson 1981; Miesch & Bally 1994; Fuller & Myers 1992; Caselli & Myers 1995). Since the total linewidths of GMCs are mostly nonthermal (the clouds are stable against gravitational collapse on the largest scales, but have masses several orders of magnitude above the thermal Jeans value, so that their support must come largely from nonmagnetic or, very likely, MHD turbulence), this decrease reflects a move towards domination by thermal motions on the smallest scales. We should therefore expect the linewidths of low-mass cores to have a smaller turbulent component than those of high-mass cores. This is indeed the case; in fact, the velocities nearest the centers of small cores are almost (to within a few percent) wholly thermal. However, it also happens (Caselli & Myers 1995) that the nonthermal velocity dispersion shows *a stronger dependence on radius in low-mass cores* (where $\sigma_{\rm NT} \propto r^{0.5}$) than in massive ones ($\sigma_{\rm NT} \propto r^{0.2}$). Because star formation is localized in the cores of GMCs, their overall structure — and this aspect specifically — bears strongly on our understanding of this most fundamental process.

The goal of this paper is to find a model for the internal structure of molecular cores (low- and high-mass both) which quantitatively matches their observed, internal velocity-dispersion profiles, and is also consistent with global properties (such as the observed mass-radius-linewidth relations) of large, self-gravitating clumps and even whole GMCs. Our approach is to reduce this problem to the specification of a (total) pressure-density relation — an equation of state — that, when used to solve the equation of hydrostatic equilibrium, results in a gas cloud with the required features. It is significant that the linewidth profiles of cores are insensitive to the presence or absence of young stars, and thus may be viewed as one of the prerequisites for star formation (Fuller & Myers 1992; Caselli & Myers 1995). This justifies our focus on the structure of purely gaseous clouds.

To proceed, we shall resort to a virial-theorem treatment of molecular clouds which idealizes them as spheres of gas in hydrostatic equilibrium and satisfying Poisson's equation. This is appropriate enough for dense cores, which in many cases are roughly spheroidal (probably prolate: Myers et al. 1991), or even near spherical (e.g., Williams et al. 1995), overall. (Although their internal density distributions may not be especially smooth on very small scales, we concern ourselves here with a description of their *bulk* structure.) In addition, observations of very massive cores imply that they are self-gravitating and in approximate "gravitational virial equilibrium," $2\,\mathcal{U} + \mathcal{W} \approx 0$. This is not the case for low-mass cores, but these still appear to satisfy the full virial theorem if surface-pressure terms are included (Bertoldi & McKee 1992). Finally, even the total masses, radii, and linewidths of entire GMC complexes are generally consistent with virial-equilibrium models of spheres (e.g., Solomon et al. 1987; Elmegreen 1989); and it has been repeatedly confirmed that whole clouds tend to comply with $2\,\mathcal{U} + \mathcal{W} \approx 0$ (Larson 1981; Solomon et al. 1987; Myers & Goodman 1988b).

It should be noted that the correct, average mass-radius and size-linewidth relations can be recovered in a purely scale-free description of GMCs (e.g., Henriksen 1991). But the distinctly different scalings of velocity dispersion with radius inside low- and high-mass clumps is one indication that molecular clouds are in fact not entirely featureless. Other current models for these objects (such as isothermal spheres or negative-index polytropes) face similar difficulties in accounting simultaneously for their global properties and their internal structures.

Magnetic fields are an important presence in regions of star formation (e.g., Heiles et al. 1993), so we begin in §2 by writing down the virial-theorem (or Bonnor-Ebert) relations between the masses and total linewidths — including turbulent velocities — of magnetized spheres, truncated at radii such that the internal pressure just balances that of a diffuse surrounding medium. We then develop a stability criterion for such clouds which depends only on the assumption that their thermal linewidths (i.e., kinetic temperatures) are invariant. When combined with the circumstantial evidence for equipartition between the kinetic and mean-field magnetic energies in GMCs and massive cores (Myers & Goodman 1988a, b; Bertoldi & McKee 1992), this stability criterion leads to mass-radius-linewidth relations between critical-mass objects that agree with the observed scalings (both the exponents and the coefficients) among GMCs. Our analysis is therefore similar to those of, e.g., Chièze (1987), Fleck (1988), and especially Elmegreen (1989), but ours holds for clouds with an *arbitrary* equation of state. In addition, we find that critically stable clouds in magnetic equipartition should all satisfy $2\,\mathcal{U}+\mathcal{W}\approx 0$. We therefore conclude that GMCs and massive cores are approximately at their critical masses and magnetically supercritical, with $M_{\rm crit}\simeq 2\,M_\Phi$ (see also McKee 1989; Bertoldi & McKee 1992). The generality of these results allows for the investigation of essentially any pressure-density relation as a potential description of the interiors of molecular cores, just so long as critically stable configurations are at all possible.

In §3, we discuss polytropic equations of state: $P\propto\rho^\gamma$, with γ any positive number. Clearly, if $\gamma\geq 1$, then the total velocity dispersion ($\sigma^2=P/\rho$) stays constant or decreases with decreasing density (increasing radius) inside a cloud. If instead γ is allowed to be less than 1 (e.g., Maloney 1988), then σ^2 increases with radius, as required. However, in our analysis, any such "negative-index" polytrope would be unconditionally stable against gravitational collapse; or equivalently (but independently of any stability criterion), it could not self-consistently satisfy the relation $2\,\mathcal{U}+\mathcal{W}\approx 0$. While this is not a problem for low-mass cores, it is inconsistent with what we know of very large clumps, and GMCs overall. Thus, we argue that polytropic pressure-density relations give an incomplete picture of interstellar clouds. A corollary to this is that weakly damped Alfvén waves, for which $P\propto\rho^{1/2}$ (McKee & Zweibel 1995), cannot be invoked as the *sole* explanation of nonthermal linewidths in GMCs.

Section 4 describes what is, in our view, a more suitable alternative. There we consider the possibility that pressure varies only logarithmically with density: $P/P_c=1+A\,\ln(\rho/\rho_c)$. We refer to the resulting gas cloud as a "pure" logotrope. This term was introduced by Lizano & Shu (1989;

see also McKee 1989), who actually added a logarithmic term to an otherwise isothermal equation of state in an attempt to account for turbulent linewidths. Such models have also been studied in detail by Gehman et al. (1996). Here, however, we dispense with the explicitly isothermal component, for two reasons: (1) Assuming $P = \rho\sigma_{\rm T}^2 + \kappa \ln(\rho/\rho_{\rm ref})$, with $\sigma_{\rm T}$ the thermal velocity dispersion and $\rho_{\rm ref}$ some reference density (Lizano & Shu 1989), the observational inference that linewidths should be essentially purely thermal at the centers of cores requires that $\rho_{\rm ref} = \rho_c$. But then the internal $\sigma^2 = P/\rho$ *decreases* with increasing radius. (2) If now $P/P_c = \rho/\rho_c + \kappa \ln(\rho/\rho_c)$, then for large values of κ such as those suggested by Gehman et al. (1996), P vanishes for ρ/ρ_c rather near unity. Thus, real clouds would have to be almost uniform-density, which again is not observed.

These difficulties do not extend to the specific equation of state which we examine. Instead, an outwards-increasing velocity-dispersion profile obtains for an equilibrium pure logotrope. Such a model can moreover account for the observed mass-radius and size-linewidth relations between GMCs. We also demonstrate that the linewidth measurements in both low- and high-mass cores, from a variety of molecular clouds, are quantitatively reproduced if $A \simeq 0.2$. The argument makes explicit use of the fact that small cores are *not* at their critical masses (while large ones generally are), but that they are still in approximate virial equilibrium when the effects of surface pressures are considered.

Although the logarithmic $P - \rho$ relation we advocate is phenomenological, its overall viability, along with the failings of other models, ultimately makes for a useful description of molecular clouds and their cores.

2. Generalized Bonnor-Ebert Relations

Interstellar clouds can be viewed as essentially "pressure-truncated" bodies of gas. (This term is meant to imply the existence, not of some radius where a gas cloud suddenly ends, but of one where it "blends in" with an ambient medium.) Thus, the boundary of a GMC is set by pressure balance with the surrounding, hot ISM. Note that even if there is no such balance initially, it will eventually obtain after an overall expansion or contraction of the cloud complex. The extent of a core within a GMC is similarly limited by the pressure of a tenuous interclump medium, as has been argued by Bertoldi & McKee (1992). The equilibrium structure of pressure-truncated isothermal spheres was first described by Ebert (1955) and Bonnor (1956) (see also McCrea 1957). Their expressions connecting the masses, radii, and linewidths of the spheres follow from the assumption of hydrostatic equilibrium and Poisson's equation, and therefore are written in terms of an internal pressure profile and gravitational potential. In Appendix A, we re-derive these Bonnor-Ebert relations, but for clouds satisfying an arbitrary gas equation of state (eqs. [A4]–[A7]). We also provide a connection (eqs. [A8]–[A10]) with the more transparent and observationally convenient virial-theorem formulation given by equations (2.8) below. As various authors have noted (Chièze 1987; Fleck 1988; Maloney 1988; Elmegreen 1989), these relations in either guise provide a framework for an understanding of the standard "Larson's laws" for GMCs ($M \propto R^2$ and $\sigma \propto R^{1/2}$; Larson 1981).

The development of Appendix A refers specifically to "nonmagnetic" clouds, meaning only that no *ordered* (mean) magnetic field is considered to be present. We work on the assumption that the effects of disordered fields (MHD turbulence) can be separately dealt with, in an equivalent hydrostatic problem that makes use of an effective equation of state to describe *all* of the contributions to gas pressure as a function of density. Still, the effects of mean fields must also be considered in any applications to real interstellar clouds.

2.1. Magnetic Equilibria

In the absence of any analytic models for magnetohydrostatic clouds, we proceed by assuming spherical symmetry and turning to the scalar virial theorem:

$$2\,\mathcal{U}(1 - P_s/P_{\rm ave}) + \mathcal{M} + \mathcal{W} \;=\; 0\;. \tag{2.1}$$

Here the mass-averaged, total one-dimensional velocity dispersion of a cloud with radius R is related to its mean pressure and density by

$$\sigma^2_{\rm ave} = \frac{\int_0^R 4\pi r^2 \rho \sigma^2\; dr}{\int_0^R 4\pi r^2 \rho\; dr} = \frac{P_{\rm ave}}{\rho_{\rm ave}}\;, \tag{2.2}$$

so that the kinetic (or internal), mean-field magnetic, and gravitational energies are given by the usual

$$\mathcal{U} = \frac{3}{2}\; M\sigma^2_{\rm ave}\;, \tag{2.3}$$

$$\mathcal{M} = \frac{1}{8\pi}\int B^2\; dV + \frac{1}{4\pi}\oint (\mathbf{r}\cdot\mathbf{B})\mathbf{B}\cdot d\mathbf{S} - \frac{1}{8\pi}\oint B^2\mathbf{r}\cdot d\mathbf{S}\;, \tag{2.4}$$

and

$$\mathcal{W} = -G\int_0^R \frac{m\; dm}{r} \equiv -\frac{3}{5}a\frac{GM^2}{R}\;. \tag{2.5}$$

The parameter a is essentially a measure of the non-uniformity of a gas sphere, and as such depends on the equation of state and the truncation radius (in terms of a fixed scale r_0; eq. [A8]). However, it is generally of order unity: for a power-law density profile $\rho \propto r^{-p}$, equation (2.5) gives $a = (1 - p/3)/(1 - 2p/5)$. We expect $1 \lesssim p \lesssim 2$ in a realistic GMC or core, and thus $10/9 \lesssim a \lesssim 5/3$.

It is often more useful to work in terms of the virial parameter of Bertoldi & McKee (1992):

$$\alpha_{\rm mag} \equiv \frac{5\sigma^2_{\rm ave}R}{GM}\;. \tag{2.6}$$

This *observable* quantity can also be written (cf. McKee & Zweibel 1992) as

$$\alpha_{\rm mag} = 2a\,\frac{\mathcal{U}}{|\mathcal{W}|} = \frac{a}{1 - P_s/P_{\rm ave}}\left(1 - \frac{\mathcal{M}}{|\mathcal{W}|}\right) \ .$$

Although this form of the virial theorem is appropriate for clouds of any shape, the corrective factors for spheroidal clouds are rather near unity (Bertoldi & McKee 1992), and we still allow only for spherical symmetry here. It is further convenient to distinguish between the virial parameters which would obtain for a cloud with and without a mean magnetic field; these are related by

$$\alpha_{\rm mag} = \alpha_{\rm non}\left(1 - \frac{\mathcal{M}}{|\mathcal{W}|}\right) \ . \tag{2.7}$$

Again, $\alpha_{\rm mag}$ refers specifically to the combination (2.6) of observables. On the other hand, $\alpha_{\rm non}$ applies to the $\mathcal{M} = 0$ (no mean field) counterpart of a given cloud; it is directly observable only in this special case (since then $\alpha_{\rm mag} = \alpha_{\rm non}$), but may always be calculated for a given gas equation of state, as outlined in Appendix A. Once this is known, $\alpha_{\rm mag}$ follows with the specification of a mean-field configuration (see §2.3).

The connection (2.7) between $\alpha_{\rm mag}$ and $\alpha_{\rm non}$ is valid insofar as the ratio $P_s/P_{\rm ave}$ does not change drastically upon the "addition" of a mean magnetic field to a cloud which is already in hydrostatic equilibrium. This must hold along field lines anyway (force balance is required in that direction), and thus everywhere on the surface of a roughly spherical cloud. Defining $a_{\rm eff} \equiv a(1 - \mathcal{M}/|\mathcal{W}|)$, such reasoning implies that $(\alpha_{\rm mag} - a_{\rm eff})/\alpha_{\rm mag} = (\alpha_{\rm non} - a)/\alpha_{\rm non}$, so manipulation of the virial theorem gives the following:

$$M = 25\sqrt{\frac{3}{20\pi}}\left(\frac{\alpha_{\rm non} - a}{\alpha_{\rm non}}\right)^{1/2}\frac{1}{\alpha_{\rm mag}^{3/2}}\,\frac{\sigma_{\rm ave}^4}{(G^3 P_s)^{1/2}} \ , \tag{2.8a}$$

$$R = 5\sqrt{\frac{3}{20\pi}}\left(\frac{\alpha_{\rm non} - a}{\alpha_{\rm non}}\right)^{1/2}\frac{1}{\alpha_{\rm mag}^{1/2}}\,\frac{\sigma_{\rm ave}^2}{(G P_s)^{1/2}} \ , \tag{2.8b}$$

$$\Sigma = \sqrt{\frac{20}{3\pi}}\left(\frac{\alpha_{\rm non}}{\alpha_{\rm non} - a}\right)^{1/2}\frac{1}{\alpha_{\rm mag}^{1/2}}\left(\frac{P_s}{G}\right)^{1/2} \ , \tag{2.8c}$$

and

$$\rho_{\rm ave} = \frac{\alpha_{\rm non}}{\alpha_{\rm non} - a}\,\frac{P_s}{\sigma_{\rm ave}^2} \ . \tag{2.8d}$$

These relations, of which only two are independent (they are contained, for example, in eqs. [9] and [10] of Elmegreen 1989), are also given by Harris & Pudritz (1994) for the specific case of critically stable isothermal spheres (as defined in §2.2; $\alpha_{\rm non} = 2.054$ and $a = 1.221$ at a cloud radius $R_{\rm crit}/r_0 = 2.150$). As written here, they apply to any generic gas cloud, stable or unstable, isothermal or not.

Any cloud in hydrostatic equilibrium and satisfying Poisson's equation has a central region where the potential, density, and velocity dispersion are very nearly constant with radius.

Equations (A8) and (A9) show that spheres truncated in or just outside this central region (i.e., at radii small enough that $P_s \approx P_c$) have $\alpha_{\rm non} \gg a$, and thus $\alpha_{\rm mag} \propto M^{-2/3} \propto R^{-2}$ by equations (2.8a, b). Roughly this scaling has been observed for the virial parameters of low-mass, high-α cores in several GMCs, leading Bertoldi & McKee (1992) to argue that such clumps can be viewed as truncated spheroids which are essentially in pressure equilibrium with an intracloud medium.

2.2. Stability: Critical Clouds

Given equations (2.8) for the equilibrium structure of pressure-truncated gas spheres, we are in a position to question their stability: Under what conditions will they be able to withstand the combined effects of self-gravity and surface pressure, and when will they be unstable to wholesale gravitational collapse? The answer to this depends, of course, on any boundary conditions attached to a perturbation of the cloud. Obviously, the total mass should be unchanged by a contraction or expansion of the entire structure. In addition, following Maloney (1988), we suppose that the central velocity dispersion remains constant as the cloud radius, or the surface pressure, is varied. This stipulation is meant to reflect the fact that the turbulent linewidth decreases steadily towards smaller scales in cores and in entire GMCs. We therefore identify the central velocity dispersion with the thermal part of the total linewidth: $\sigma_c^2 = kT/\mu m_H$. Insisting that this be invariant amounts to recognizing the rough uniformity of kinetic temperatures $T \sim 10K$ (which to first order can be understood as a consequence of the competition between cosmic-ray heating and CO cooling) over a large range of scales in interstellar clouds. The stability criterion that follows ultimately leads to a set of results which self-consistently explain some important observational features of GMCs and massive cores.

A gas cloud will be stable against radial perturbations if the derivative $\partial P_s/\partial R$ (taken with σ_c and M held fixed) is ≤ 0: a slight decrease in the cloud radius then leads to an increase in the pressure just inside its boundary, which in turn leads to reexpansion. Appendix B shows that, for any equation of state, this condition is just

$$\left(\frac{\partial P_s}{\partial R}\right)_{M,\sigma_c} = -6\frac{P_s}{R}\left[\frac{1-(5/6)(\alpha_{\rm non}-a)^{-1}}{3-\rho_{\rm ave}/\rho_s}\right] \leq 0 \ , \qquad (2.9)$$

where ρ_s is the internal density at the edge of the cloud. Although this stability criterion has been derived without explicitly considering the effects of mean magnetic fields, we expect that it should not be greatly altered by their inclusion. (This is again implied by our assumption of approximate spherical symmetry, since eq. [2.9] must at least be satisfied along field lines at the boundary of a magnetized cloud.)

Depending on the equation of state, there may exist a radius for which a pressure-truncated cloud is marginally stable (the expression [2.9] is just 0), and beyond which it is unstable. It is these critical equilibria, which must have

$$\alpha_{\rm non} - a = \frac{5}{6} \ , \tag{2.10}$$

that are of particular interest here. Once $\alpha_{\rm non}$ and a are known as functions of radius (as in Appendix A), the satisfaction, if possible, of equation (2.10) sets the boundary $R_{\rm crit}/r_0$ of the cloud. This in turn allows for evaluation of the coefficients in equations (2.8). Quite generally,

$$M_{\rm crit} = \frac{25}{\sqrt{8\pi}} \, \frac{1}{\alpha_{\rm non}^{1/2}\alpha_{\rm mag}^{3/2}} \, \frac{\sigma_{\rm ave}^4}{(G^3 P_s)^{1/2}} \ , \tag{2.11a}$$

$$R_{\rm crit} = \frac{5}{\sqrt{8\pi}} \frac{1}{\alpha_{\rm non}^{1/2}\alpha_{\rm mag}^{1/2}} \, \frac{\sigma_{\rm ave}^2}{(G P_s)^{1/2}} \ , \tag{2.11b}$$

$$\Sigma_{\rm crit} = \sqrt{\frac{8}{\pi}} \, \left(\frac{\alpha_{\rm non}}{\alpha_{\rm mag}}\right)^{1/2} \left(\frac{P_s}{G}\right)^{1/2} \ , \tag{2.11c}$$

and

$$\rho_{\rm ave,crit} = \frac{6\alpha_{\rm non}}{5} \, \frac{P_s}{\sigma_{\rm ave}^2} \ . \tag{2.11d}$$

Equation (2.11c) shows that a nonmagnetic cloud ($\alpha_{\rm mag} = \alpha_{\rm non}$) on the verge of gravitational collapse has a mean column density which is fixed by the pressure of the surrounding medium, independently of any gas equation of state.

In general, the virial parameter of a given cloud is sensitive to its internal structure (through the equation of state) and its total radius. However, for a *critically stable* cloud we always have $\alpha_{\rm non} = a + 5/6$. Since a is typically of order (but slightly greater than) unity, this implies $\alpha_{\rm non} \approx 2$ and $1 - P_s/P_{\rm ave} = a/\alpha_{\rm non} \approx 1/2$. The virial theorem (2.1) then becomes

$$\mathcal{U} + \mathcal{M} + \mathcal{W} \approx 0 \ . \tag{2.12}$$

If there is equipartition $\mathcal{M} \approx \mathcal{U}$ between the magnetic and kinematic energies in such a cloud, then $2\,\mathcal{U} + \mathcal{W} \approx 0$ as well; thus, $\mathcal{M}/|\mathcal{W}| \approx 1/2$, and the critical $\alpha_{\rm mag}$ is expected to be of order unity (cf. eq. [2.7]; see also Elmegreen 1989 and McKee & Zweibel 1992).

Observations of molecular clouds show that $2\,\mathcal{U} + \mathcal{W} \approx 0$ (or equivalently, $\alpha_{\rm mag} \approx 1$), and are *consistent* with $\mathcal{M} \approx \mathcal{U}$ (Myers & Goodman 1988a, b), although actual magnetic-field measurements are few and uncertain. The most massive cores in GMCs similarly tend to show $2\,\mathcal{U} + \mathcal{W} \approx 0$ and $\alpha_{\rm mag}$ near 1 (this is not the case for low-mass cores, however: e.g., Williams, de Geus, & Blitz 1994; Williams et al. 1995; see also §4.1 below). Observations of them are also indicative of magnetic equipartition (Bertoldi & McKee 1992), though again the evidence is rather indirect, and not necessarily conclusive. Having said this, it does seem that GMCs and massive cores both satisfy equation (2.12), which would imply that they are at or near their critical masses.

Thus arrived at, this conclusion depends on the criterion one adopts for cloud stability, i.e., it follows from the assumption that the thermal linewidth σ_c is held fixed during any radial perturbation (and from the additional proviso that $\mathcal{M} \approx \mathcal{U}$). Nevertheless, our analysis — which specifies no equation of state — provides a natural explanation for the fact that so many GMCs and large cores appear to be in simple "gravitational virial equilibrium" (i.e., $2\,\mathcal{U} + \mathcal{W} \approx 0$), even though they are threaded by appreciably strong mean magnetic fields.

There is also separate evidence for the criticality of massive molecular cores. For instance, Bertoldi & McKee (1992), in their study of the cores in four GMCs, argue that the most massive are at least magnetically supercritical, a necessary condition for gravitational instability. More fundamentally, star-forming regions clearly must be susceptible to gravitational collapse; but in the Rosette GMC at least, those cores which are most obviously associated with IRAS sources are also among the heaviest (Williams et al. 1995). As mentioned above, the largest cores in several GMCs also have the smallest virial parameters (as low as 1), so that this would seem to be a feature of clouds which are close to instability. The observation of a mean $\alpha_{\rm mag} \approx 1$ for GMCs then implies that they, too, are near some critical mass, and certainly in excess of the nonmagnetic Jeans or Bonnor-Ebert value (for which $\mathcal{M} = 0$ implies $\mathcal{U} + \mathcal{W} \approx 0$ and $\alpha_{\rm mag} = \alpha_{\rm non} \approx 2$). McKee (1989) has further argued that GMCs on the whole are magnetically supercritical, and of course they must be strongly self-gravitating in order to be molecular at all (e.g., Elmegreen 1985).

On a related note, McKee (1989) points out that GMCs must generally be near criticality because they show a $P_{\rm ave}$ which is typically an order of magnitude larger than the total (thermal plus turbulent) pressure in the hot ISM. Given our stability criterion, equation (2.11d) shows that self-gravity can supply a maximal pressure enhancement $P_{\rm ave}/P_s \approx 2.5$ of a spherical cloud over its surrounding medium, and this only for a critical-mass body. Even putting the nonsphericity of GMCs aside, however, it is important to note that the analysis here speaks only to the molecular, self-gravitating parts of GMCs, and not to their diffuse, low-A_V H I components. Elmegreen (1989) has shown that the weight of these atomic "envelopes" can easily increase the pressure at the boundaries of the molecular parts of a cloud complex by a factor of 5 or more above the value in the ISM at large; overall, then, $P_{\rm ave}/P_{\rm ISM} > 10$.

If GMCs and their most massive cores are indeed critical-mass objects, then they must all have the same dimensionless radii (although the physical scale r_0 will generally vary), and the same virial parameters. Aside from possible variations in P_s, which are discussed in detail by Elmegreen (1989), this causes the coefficients in equations (2.11) or (2.8) to be roughly constant, and allows for well defined mass-radius-linewidth relations between clouds. Moreover, we have argued that $\alpha_{\rm non} \simeq 2$ and, in the event of magnetic equipartition, $\alpha_{\rm mag} \simeq 1$ for critical clouds, regardless of the underlying equation of state. The coefficients in the $M - R - \sigma_{\rm ave}$ scalings are then independent of this detail, and the average properties of GMCs can shed no light on their internal structure. This both explains why critical, magnetized isothermal-sphere models are successful in quantitatively accounting for the observed scalings (with $\alpha_{\rm non} = 2.054$ and $\alpha_{\rm mag} \simeq 1$: Elmegreen 1989; Harris & Pudritz 1994), and implies that the same agreement with the data comes with *any* model which provides for the existence of a critical mass (see eqs. [4.12] below).

Finally, equations (2.11) as written would suggest that all GMCs must be under similar surface pressures P_s if, for example, Σ is to be roughly the same among them. Other authors (e.g., McKee 1989; Mouschovias 1987; Myers & Goodman 1988b) have argued instead that either Σ itself (and hence $P_{\rm ave}$), or the mean field strength $B_{\rm ave}$, is the more fundamentally invariant attribute of GMCs. If so, then P_s could be eliminated from the critical Bonnor-Ebert relations in favor of any of these quantities, and our approach does not preclude the others.

2.3. Magnetic Field Model

Consider a cloud of radius R, threaded by a mean magnetic field approximated as uniform and of magnitude $B_{\rm ave}$. Outside the cloud, let B fall off as r^{-2} to a radius R_0, where it matches onto an ambient, uniform field of strength B_0 (Nakano 1984). Conservation of flux (or continuity of the normal component of $\mathbf{B}$ across the boundary of the cloud) demands $B_{\rm ave}R^2 = B_0R_0^2$, and evaluating equation (2.4) at the surface $r = R_0$ gives

$$\mathcal{M} = \frac{B_{\rm ave}^2 R^3}{3}\left(1 - \frac{R}{R_0}\right) .$$

Defining $\beta = 8\pi P_{\rm ave}/B_{\rm ave}^2$ and $\Phi = \pi B_{\rm ave}R^2$, we have

$$\frac{\mathcal{M}}{|\mathcal{W}|} = \frac{5}{9a\pi^2}\,\frac{\Phi^2}{GM^2}\left(1 - \frac{R}{R_0}\right) = \frac{2\alpha_{\rm mag}}{3a\beta}\left(1 - \frac{R}{R_0}\right) , \qquad (2.13)$$

so that equation (2.7) gives

$$\frac{1}{\alpha_{\rm mag}} = \frac{1}{\alpha_{\rm non}} + \frac{2}{3a\beta}\left(1 - \frac{R}{R_0}\right) . \qquad (2.14)$$

With $B_0 \simeq 3\ \mu$G and $B_{\rm ave} \simeq 30 - 40\ \mu$G for GMCs (Myers & Goodman 1988b), flux conservation gives $R/R_0 \simeq 0.3$; and $\mathcal{U} \simeq \mathcal{M}$ implies $\beta \simeq 1$. Thus, $\alpha_{\rm mag} \approx 1$ when $\alpha_{\rm non} \approx 2$, as expected.

Some indication of the reliability of equations (2.11) and (2.13), and of the approximations leading to them, can be had by comparing the critical masses they predict for magnetized, isothermal spheres ($a = 1.221$) with those obtained from self-consistent, axisymmetric numerical calculations. In particular, the mass M_Φ which separates magnetically sub- and supercritical clouds, and for which $\mathcal{M} = |\mathcal{W}|$, is given by equation (2.13) as $0.18\ \Phi/G^{1/2}$, only a 50% overestimate of the exact result $M_\Phi \simeq 0.12\ \Phi/G^{1/2}$ (Mouschovias & Spitzer 1976; Tomisaka, Ikeuchi, & Nakamura 1988). Further, for $M \gtrsim 0.24\ \Phi/G^{1/2}$, the critical masses we obtain by using equation (2.7) in (2.11a) lie within a factor 2 of those found by Tomisaka et al. (1988; see their eq. [4.7]). (In fact, our formula is more accurate in the weak-field limit because it approaches the correct $M_{\rm crit} = 1.182\ \sigma^4/(G^3P_s)^{1/2}$ for the nonmagnetic, $\Phi = 0$ isothermal sphere.) And for the equipartition $\beta = 1$ seen in GMCs, setting $\alpha_{\rm mag} \approx 1$ in equation (2.13) implies $M_{\rm crit} \approx (5/6\pi^2)^{1/2}\Phi/G^{1/2}$. This is roughly 1.6 times our (approximate) M_Φ, and 2.4 times the exact value, which level of agreement is quite acceptable. In any case, we are led to expect that critical-mass GMCs and cores are strongly magnetically supercritical, with $M_{\rm crit} \approx 2\ M_\Phi$ — a result which has also been argued by McKee (1989) and Bertoldi & McKee (1992).

3. Polytropic Equations of State

The outwards increase of linewidth both within giant molecular clouds as a whole (Larson 1981; Miesch & Bally 1994) and within individual dense cores (Fuller & Myers 1992; Caselli & Myers 1995), immediately suggests the class of negative-index polytropes as possible models for these structures. That is, if $P \propto \rho^{1+1/N}$, then for a polytropic index $N < -1$ we have P/ρ increasing for decreasing ρ, as required. Such models have been studied by, e.g., Viala & Horedt (1974) and Maloney (1988), and we derive the generalized Bonnor-Ebert relations for them in Appendix C. Although there are various physical arguments to support their use (e.g., Shu et al. 1972; de Jong, Dalgarno, & Boland 1980; McKee & Zweibel 1995), these polytropes turn out to be unlikely descriptions of real GMCs (and of course, a positive polytropic index is undesirable because it is inconsistent with a velocity dispersion that increases with radius).

Here we define $n = N/(N+1)$, so that $P \propto \rho^{1/n}$ and $n > 1$ for $N < -1$. From Appendix C, a nonmagnetic, negative-index polytrope which is truncated anywhere outside of its constant-density central region (inside which, $a \simeq 1$ and $\alpha_{\rm non}$ increases without bound towards $r = 0$) will then satisfy

$$\alpha_{\rm non} - a = \frac{5}{6}(4n-3) \ .$$

Thus, an $n > 1$ polytrope has $(5/6)(\alpha_{\rm non} - a)^{-1} < 1$; and since its density profile is $\rho \propto r^{-p}$, with $p < 2$ everywhere for any n (Appendix C), we also find $\rho_{\rm ave}/\rho_s < 3$. According to equation (2.9), then, *a truncated, negative-index polytrope will always be stable, and never critically so* (as was also noted by Maloney 1988). Ultimately, the same steady increase of linewidth with radius which would recommend the polytropic equation of state in the first place also proves to be its undoing: the internal pressure gradient which results is so shallow as to stabilize a cloud under any external pressure. The concept of a critical mass is then irrelevant for these models, which casts doubt on their utility in describing real GMCs or high-mass cores. Any additional support from a mean magnetic field in the cloud obviously serves only to exacerbate this problem.

Again, this result follows to some extent from the constraint that the thermal linewidth σ_c be fixed during a perturbation of the cloud. By contrast, both Viala & Horedt (1974) and Chièze (1987) consider the possibility that the constant of proportionality in the relation $P \propto \rho^{1/n}$ is invariant, and find that polytropes can become unstable for certain truncation radii. Still, our approach is closely related to a point which is *independent of any rule for cloud stability*:

The minimum value of the nonmagnetic virial parameter for a truncated polytrope is (eq. [C7])

$$\alpha_{\rm non} \geq \frac{5}{2} \, \frac{(4n-3)(2n-1)}{6n-5} \ .$$

As usual, this is a lower limit because $\alpha_{\rm non}$ can be very large indeed if the polytrope is truncated at a very small radius. In the event of equipartition $\mathcal{U} = \mathcal{M}$ between kinematic and magnetic energies, equation (2.7) and the identity $\alpha_{\rm mag} = 2a\,\mathcal{U}/|\mathcal{W}|$ lead to

$$\alpha_{\rm mag} = \frac{\alpha_{\rm non}}{1 + \alpha_{\rm non}/(2a)} = \frac{\alpha_{\rm non}}{1 + (1/2)(1 - P_s/P_{\rm ave})^{-1}} \ ,$$

in which case equation (C11) and $n > 1$ finally imply that

$$\alpha_{\rm mag} \geq 10\ \frac{(4n-3)(2n-1)}{(6n-5)(6n+1)} > \frac{10}{7}\ .$$

Thus, regardless of whether there exist any unstable modes for truncated polytropes, the virial parameters of such clouds are significantly larger than the $\alpha_{\rm mag} \simeq 1$ $(2\,\mathcal{U} + \mathcal{W} \approx 0)$ seen in GMCs (Myers & Goodman 1988b) and in the most massive molecular cores (Bertoldi & McKee 1992; Williams et al. 1994, 1995), even if dynamically significant mean magnetic fields are allowed to be present. It is a property of our specific stability criterion that this fact implies the absence of critically stable equilibria.

The virial parameters of magnetized polytropes could be reduced to $\alpha_{\rm mag} \simeq 1$, for any n, if the mean field were such that $\mathcal{M} \simeq 2\,\mathcal{U}$. In this case, however, using equation (C11) for $P_s/P_{\rm ave}$ in the virial theorem (2.1) leads to $0.8 < \mathcal{M}/|\mathcal{W}| < 1$ for $n \geq 2$, which is difficult to reconcile with the rather higher degree of magnetic supercriticality that is observationally inferred for GMCs and massive cores ($\mathcal{M}/|\mathcal{W}| \lesssim 0.5$, and $M \simeq 2M_\Phi$; see §§2.2, 2.3).

One consequence of all of this is that the nonthermal linewidths in GMCs, $\sigma^2_{\rm NT} = \sigma^2_{\rm ave} - kT/\mu m_H$, cannot be attributed entirely to the pressure of weakly damped Alfvén waves, for which $P \propto \rho^{1/2}$ ($n = 2$, or $N = -2$; McKee & Zweibel 1995), and thus $\alpha_{\rm mag} \gtrsim 1.65$ under magnetic equipartition. It seems almost certain that Alfvén waves do play a significant role in the support of GMCs and cores (e.g., Arons & Max 1975; Pudritz 1990); but, as McKee & Zweibel (1995) also note, they cannot be uniquely responsible for their large-scale stability. In this context, we note that the size-linewidth relation between clouds can be expressed in terms of a mean magnetic field strength, as in, e.g., Myers & Goodman (1988a). Specifically, equation (2.11d) can be used to write (2.11b) in terms of $P_{\rm ave}$ rather than P_s, and the definition of β (§2.3) relates $P_{\rm ave}$ to $B_{\rm ave}$. Then, with a mean mass per particle $\mu = 2.33$ and a kinetic temperature $T = 10$ K, we have

$$\sigma_{\rm NT} \simeq 0.60\ {\rm km\ s^{-1}}\ (\alpha_{\rm mag}\beta)^{1/4} \left(\frac{B_{\rm ave}}{30\ \mu{\rm G}}\right)^{1/2} \left(\frac{R}{1\ {\rm pc}}\right)^{1/2}\ .$$

The equality is not quite exact here, because the scalings with $B_{\rm ave}$ and R strictly apply to the total $\sigma_{\rm ave}$. Still, this relation is accurate in the typical case, $\sigma^2_{\rm NT} \gg kT/\mu m_H$; and for $\alpha_{\rm mag} = \beta = 1$, it is consistent with available data (see Myers & Goodman 1988a). Thus, although Mouschovias & Psaltis (1995) argue for an interpretation of this result in terms of Alfvén waves, we see here that it is independent of *any* assumptions on the physical origin of the nonthermal motions in GMCs (in principle, they need not even derive from magnetic fields).

Finally, it is clear that any simple “mixing” of two polytropes with different indices will still preclude the existence of a critical (or low-$\alpha_{\rm mag}$) cloud; even the superposition of an isothermal part, i.e., $P = C_1\rho + C_2\rho^{1/n}$, only admits one if it is essentially isothermal anyway ($C_1 \gg C_2$). Thus, we now turn to a different equation of state, in which the gas pressure varies only logarithmically with density.

4. The Logotrope

Many theoretical models of star-forming clouds employ the singular isothermal sphere, in which $\rho \propto r^{-2}$. However, there is some evidence that H II regions are concentrated towards the CO centroids of their parent GMCs such that their three-dimensional number density is most consistent with an r^{-1} fall-off (Waller et al. 1987; Scoville et al. 1987). This suggests the possibility that, in a heavily smoothed, average sense, the internal density structure of molecular clouds is essentially $\rho \propto r^{-1}$ (see also Solomon et al. 1987). Further, extinction measurements indicate $\rho \propto r^{-1}$ or so in the outer parts of cores as well (Cernicharo, Bachiller, & Duvert 1985; Stüwe 1990).

Lizano & Shu (1989; see also Gehman et al. 1996) introduced the so-called logotropic equation of state for GMCs, $P = P_{\rm iso} + P_{\rm turb}$, with $P_{\rm iso} \propto \rho$ and $P_{\rm turb} \propto \ln(\rho/\rho_{\rm ref})$. If the central linewidth of a cloud is to be entirely thermal in origin, the reference density in $P_{\rm turb}$ must be $\rho_{\rm ref} = \rho_c$. However, P/ρ then *decreases* with radius, which is incompatible with the observations. We suggest that a more complete description of GMCs and cores is given instead by a "pure" logotrope:

$$P = \rho_c \sigma_c^2 \left[1 + A \ln\left(\frac{\rho}{\rho_c}\right)\right] \ , \tag{4.1}$$

with $A > 0$ a parameter to be adjusted. The assumption here is that any nonthermal motions, which presumably arise from MHD turbulence, add to the thermal pressure such that both are fully accounted for by the equation of state (4.1). This relation is shown schematically in Fig. 1, along with an isothermal-sphere combination and the polytropic $P \propto \rho^{1/2}$ for Alfvén waves. In the rest of our discussion, equation (4.1) is referred to simply as a logotrope, with the understanding that no further consideration is given to any mixed-isothermal version.

Given equation (4.1), the equation of hydrostatic equilibrium (A1) integrates to

$$\frac{\rho}{\rho_c} = \frac{1}{1 + \psi/A} \ , \tag{4.2}$$

where $\psi = (\phi - \phi_c)/\sigma_c^2$ is a dimensionless gravitational potential. Substitution of this expression into Poisson's equation (A2) shows the existence of a singular solution,

$$\frac{\rho}{\rho_c} = \sqrt{\frac{2A}{9}} \left(\frac{r}{r_0}\right)^{-1} \ , \tag{4.3}$$

which describes the density profile of the bounded (finite ρ_c) solution at large radii. (The scale radius $r_0 = 3\sigma_c/[4\pi G \rho_c]^{1/2}$.) In spite of such a slowly decreasing internal density, a logotrope has only a finite extent, since for any positive A the pressure will eventually vanish. Assuming that A is *small* enough for the singular density profile to apply at the edge of the cloud, we have

$$\xi_{\rm max} = \frac{R_{\rm max}}{r_0} = \sqrt{\frac{2A}{9}} \, e^{1/A} \ . \tag{4.4}$$

The velocity dispersion, $\sigma^2 = P/\rho$, increases with radius inside the cloud until it reaches a maximum of

$$\sigma^2_{\rm max}/\sigma^2_c = Ae^{1/A-1} \tag{4.5}$$

at $\xi = r/r_0 = e^{-1}\xi_{\rm max}$, beyond which it falls again (to 0, at $\xi_{\rm max}$).

A logotrope truncated by the pressure P_s of an external medium has precisely one critical mode for any given value of A. As discussed in Appendix B, if a cloud is truncated at a very small radius ξ, it will always be stable. But in the power-law part of the logotrope, equations (4.2) and (4.3) show that $d\psi/d\xi = (9A/2)^{1/2}$, so once ξ is so large that $P_s/P_c < A/4$, the cloud is unstable (cf. eq. [B6]). Thus,

$$\xi_{\rm crit} = \frac{R_{\rm crit}}{r_0} = \sqrt{\frac{2A}{9}}\,\exp\left(\frac{1}{A}-\frac{1}{4}\right) = e^{-1/4}\xi_{\rm max}\ , \tag{4.6}$$

where we have again assumed that A is relatively small and the singular solution (4.3) holds at $\xi_{\rm crit}$. (This expression shows that σ achieves its maximum *inside* $\xi_{\rm crit}$, and the surface of the critical logotrope is cooler than its interior. McKee [1989] has suggested that such behavior might arise from the radiation of Alfvén waves into the ambient medium.) Now, evaluating the pressure (4.1) and density (4.3) at the radius (4.6) yields, for any critically stable logotrope,

$$\left(\frac{\rho_s}{\rho_c}\right)_{\rm crit} = \exp\left(\frac{1}{4}-\frac{1}{A}\right) \qquad \left(\frac{\sigma_s^2}{\sigma_c^2}\right)_{\rm crit} = \frac{A}{4}\,\exp\left(\frac{1}{A}-\frac{1}{4}\right) \qquad \left(\frac{P_s}{P_c}\right)_{\rm crit} = \frac{A}{4}\ . \tag{4.7}$$

Evidently, self-consistency in the use of equation (4.3) here requires $A \ll 4$. Equations (A7) and (2.2) can then be used to find

$$\left(\frac{\rho_{\rm ave}}{\rho_s}\right)_{\rm crit} = \frac{3}{2} \qquad \left(\frac{\sigma^2_{\rm ave}}{\sigma^2_s}\right)_{\rm crit} = \frac{14}{9} \qquad \left(\frac{P_{\rm ave}}{P_s}\right)_{\rm crit} = \frac{7}{3}\ , \tag{4.8}$$

independently of A.

A numerical solution for our logotrope with $A = 0.18$ (which we justify shortly) yields the internal density, pressure, and velocity-dispersion profiles shown in Fig. 2. Equations (4.4) and (4.6) are valid here, as an r^{-1} density profile is realized well before the cloud ends (the vertical line in all four panels of the Figure marks the radius $\xi_{\rm crit}$). It is the steep pressure gradient near $\xi_{\rm max}$ which sets the logotrope apart from the negative-index polytropes and allows for a critical cloud with a small virial parameter.

The *total* velocity dispersion σ^2 in Fig. 2 is roughly constant near the center of the cloud; and its rise with radius further on is consistent with $\sigma^2 \propto r^{2/3}$, which is essentially the scaling originally found for GMCs by Larson (1981). Identifying the central dispersion σ_c with the thermal part of the linewidth (so that thermal motions dominate on the smallest scales, as is observed), the nonthermal contribution to cloud support is $\sigma^2_{\rm NT} = \sigma^2 - \sigma^2_c$, which is also shown in Fig. 2. At small to moderate radii, $\sigma_{\rm NT}$ naturally rises more steeply than the total σ, while at larger ξ the two are more comparable in magnitude. Roughly, then, our model has $\sigma^2_{\rm NT} \propto r$ over some range in radius before it flattens to $\sigma_{\rm NT}^2 \propto r^{1/2}$ and eventually turns over (the maximum $\sigma_{\rm NT}^2/\sigma_c^2$ is just $\sigma_{\rm max}^2/\sigma_c^2 - 1$, and occurs at $\xi = e^{-3/4}\xi_{\rm crit}$). It is found that $\sigma_{\rm NT} \propto r^{0.5}$ within GMCs (e.g., Myers & Goodman 1988b), and low-mass molecular cores show the same general trend; high-mass cores are more suggestive of $\sigma_{\rm NT} \propto r^{0.25}$ (Fuller & Myers 1992; Caselli & Myers 1995). A logotropic equation of state both for individual cores and for entire cloud complexes is consistent with these observations, provided that low-mass cores can be viewed as spheres which are pressure-truncated at radii $\xi < \xi_{\rm crit}$. We discuss this point further in §4.1 below. As always, though, no matter how σ varies with r internally, the *average* relation $\sigma_{\rm ave} \propto R^{1/2}P_s^{1/4}$ still holds for critical-mass clouds, i.e., for GMCs.

A handle on an appropriate value of the parameter A for GMCs as a whole, can be gotten by reinventing them as smoothed-out spheres with a number of distinct overdense regions (the cores) sprinkled throughout. The observed contrasts in mean density and velocity dispersion between GMCs and cores can then be related to the A of a model logotrope. Harris & Pudritz (1994; see their Table 2) list each of $\rho_{\rm ave}$, $\sigma_{\rm ave}$, and Σ for a GMC of mass $\overline{M}_{\rm GMC} = 3.3 \times 10^5\ M_\odot$ and a core with $\overline{M}_{\rm core} = 5.4 \times 10^2\ M_\odot$. (Such values are "typical" in the sense that, *by mass*, half of all GMCs [cores] are larger than $\overline{M}_{\rm GMC}$ [$\overline{M}_{\rm core}$].) Defining $\widetilde{\rho}$, $\widetilde{\sigma}$, and $\widetilde{\Sigma}$ as the core-to-GMC ratios of mean volume densities, linewidths, and column densities, these data show that

$$\widetilde{\rho} \simeq 240 \qquad \widetilde{\sigma} \simeq 0.29 \qquad \widetilde{\Sigma} \simeq 4.64\ . \tag{4.9}$$

Cores with $M = \overline{M}_{\rm core}$ are among the most massive observed, and are likely near critical. If they are also logotropes, then their $\rho_{\rm ave}/\rho_s$, etc., should be roughly given by equation (4.8), regardless of whether $A_{\rm GMC} = A_{\rm core}$. Such large cores might further be expected to lie in very dense, cold, highly pressured regions of their parent clouds. Then the pressure P_s at the surface of a core is comparable to the GMC's P_c, and similarly for the density and velocity dispersion. These assumptions, together with the relation $\Sigma \propto P_s^{1/2}$ (eq. [2.11c]), result in

$$\widetilde{\rho} \simeq \left(\frac{\rho_c}{\rho_s}\right)_{\rm GMC} \qquad \widetilde{\sigma} \simeq \left(\frac{\sigma_c}{\sigma_s}\right)_{\rm GMC} \qquad \widetilde{\Sigma} \simeq \left(\frac{P_c}{P_s}\right)_{\rm GMC}^{1/2}\ . \tag{4.10}$$

Comparison of equations (4.9) and (4.7) then shows that the observed $\widetilde{\rho}$, $\widetilde{\sigma}$, and $\widetilde{\Sigma}$ (only two of which are actually independent) are realized in a logotropic GMC with

$$A_{\rm GMC} \simeq 0.175\ . \tag{4.11}$$

Although this procedure is highly idealized, it is perhaps telling that an A exists at all which gives at once the correct $\widetilde{\rho}$ and $\widetilde{\sigma}$. The logotrope appears to be the simplest barotropic equation of state which can account for these ratios *and* the small virial parameters (or the critical equilibrium) of GMCs and massive cores. For example, if GMCs and large cores were both $n = 2$ polytropes truncated at $\xi = r/r_0 \simeq 21.4$, then equation (4.9) could be roughly satisfied, but they would also have a large $\alpha_{\rm non} = 5.37$, and hence $\alpha_{\rm mag} \simeq 1.75$ for magnetic equipartition (again, $\mathcal{M} \simeq 2\,\mathcal{U}$ is required to reduce $\alpha_{\rm mag}$ to unity for a negative-index polytrope, but this is not wholly satisfactory for other reasons; see §3). Alternatively, adding an explicit $\rho^{1/2}$ term to equation (4.1) destroys the *simultaneous* correspondence between $\widetilde{\rho}$ and $\widetilde{\sigma}$ for critical clouds.

To this point, we have not accounted for any mean magnetic fields in GMCs and cores. However, these should have no effect on our estimate of $A_{\rm GMC}$ insofar as very massive clumps have the same $\alpha_{\rm mag} \approx 1$ as their parent clouds. More important is the assumption that the cores here lie at the rare, highest-pressure peaks of cloud complexes; if instead they are found in less extreme regions, then equation (4.11) is an upper limit to $A_{\rm GMC}$. Even so, more direct estimates of $A_{\rm GMC}$ are in fairly good agreement with the representative value quoted above. For example, equations (4.7) and (4.8) can be combined to obtain an expression for $\sigma_{\rm ave}^2/\sigma_c^2$; comparison with observed values of the total $\sigma_{\rm ave}$ and the thermal σ_c in GMCs then suggests $0.12 \lesssim A_{\rm GMC} \lesssim 0.16$.

On a final note, since $\rho \propto r^{-1}$ at the edges of such logotropes, we have $a = (1-1/3)/(1-2/5) = 10/9$. With the ratio of mean kinematic and magnetic pressures $\beta \simeq 1$, equations (2.10) and (2.14) then give for the critical virial parameters,

$$\alpha_{\rm non} = 35/18 \qquad \text{and} \qquad \alpha_{\rm mag} \simeq 1.07.$$

These are near 2 and 1, as expected from general arguments, and not far from the values 2.054 and 1.15 for a Bonnor-Ebert isothermal sphere. As alluded to earlier (§2.2), the mass-radius and size-linewidth relations among real GMCs can therefore be understood in terms of this model: equations (2.11b, c) become

$$\frac{M}{R^2} = 147\ M_\odot\ {\rm pc}^{-2}\ \left(\frac{P_s}{P_{\rm ISM}}\right)^{1/2} \left(\frac{P_{\rm ISM}}{10^4\ k\ {\rm cm}^{-3}\ {\rm K}}\right)^{1/2} \tag{4.12a}$$

and

$$\frac{\sigma_{\rm ave}}{R^{1/2}} = 0.37\ {\rm km\ s}^{-1}\ {\rm pc}^{-1/2}\ \left(\frac{P_s}{P_{\rm ISM}}\right)^{1/4} \left(\frac{P_{\rm ISM}}{10^4\ k\ {\rm cm}^{-3}\ {\rm K}}\right)^{1/4}\ , \tag{4.12b}$$

which agree well with observations (cf. Elmegreen 1989). Here P_s is the surface pressure on the *molecular part* of the GMC, while $P_{\rm ISM}$ is the total pressure of the hot, intercloud medium. The ratio of these two is typically around $5-10$, due to the weight placed on a GMC by its UV-shielding atomic layer (Elmegreen 1989; also §2.2 above).

4.1. Comparison With Data: Molecular Cloud Cores

As a class, dense molecular cores seem somewhat more heterogeneous than their parent GMCs. First, many studies (Carr 1987; Loren 1989; Stutzki & Güsten 1990; Lada, Bally, & Stark 1991) show that the size-linewidth relation between cores can be significantly weaker than the virial, $\sigma_{\rm ave} \propto R^{1/2}$ scaling among GMCs, and in some cases is difficult to discern at all. Second, in the L1630 GMC at least, the size-linewidth relation is considerably better defined for clumps which stand out more strongly against the interclump medium (see the comparison in Fig. 13 of Lada et al. between their "5σ" and "3σ" cores). And third, the virial parameters $\alpha_{\rm mag}$ of GMC cores are not restricted to values near 1, but rather can range as high as ≈100 (Bertoldi & McKee 1992; Williams et al. 1994, 1995).

This last point is particularly significant because the virial parameters of cores in a number of different clouds are seen to correlate with their size: low mass goes along with rather large $\alpha_{\rm mag}$, and high mass with more moderate $\alpha_{\rm mag} \approx 1$. Thus, as Bertoldi & McKee (1992) argue, the smallest clumps in GMCs are far removed from gravitational instability (surface pressure is more important than self-gravity in their confinement), while the largest are actually near criticality (strongly self-gravitating; see also §2.2 above). Equivalently, a range in the masses of cores can be viewed, at least roughly, as a range in the dimensionless radii ξ — small for low mass, and near $\xi_{\rm crit}$ for high mass — at which they are truncated by the ambient pressure in a GMC (virial parameters generally decrease with ξ for any equation of state; Appendix A). This notion could account for the rather confused size-linewidth relation *between* cores (if ξ does not have a fixed value, then neither do $\alpha_{\rm non}$ and $\alpha_{\rm mag}$ in eq. [2.8b]), and ultimately must also have consequences for the interpretation of data on the radial variation of velocity dispersion *inside* cores.

If indeed very low-mass cores differ from very high-mass ones mainly in being truncated at $\xi_{\rm low} \ll \xi_{\rm high} \simeq \xi_{\rm crit}$, then the former must be less centrally condensed, have ratios P_s/P_c nearer unity, and be generally less distinguishable from the intercore (GMC) gas than the latter. This results in the scale radius $r_0 = 3\sigma_c/(4\pi G\rho_c)^{1/2} \propto \sigma_c^2/P_c^{1/2}$ being *larger* for less massive clumps. To see this, compare the r_0 of a low-mass core, truncated at ξ small enough that $P_s \approx P_c$, with the r_0 of a near-critical, high-mass core. On average, any two cores should be under similar surface pressures P_s (this essentially being set by the internal $P_{\rm ave}$ of a parent GMC), so that

$$\frac{r_0({\rm high})}{r_0({\rm low})} \simeq \left(\frac{P_s}{P_c}\right)^{1/2}_{\rm high} \left[\frac{\sigma_c^2({\rm high})}{\sigma_c^2({\rm low})}\right] \simeq \sqrt{\frac{A}{4}} \left[\frac{\sigma_c^2({\rm high})}{\sigma_c^2({\rm low})}\right] , \qquad (4.13)$$

where the second step follows from equation (4.7) if a logotropic equation of state applies. Thus, for σ_c not too widely different between the two cores, and for A small enough, the ratio (4.13) will be < 1. The same *physical* radius r in high- and low-mass cores then corresponds to respectively larger and smaller $\xi = r/r_0$. This result, which just reflects the fact that more strongly self-gravitating structures are more centrally concentrated, must be considered when attempting to match any model to any observations.

Returning now to the issue of internal velocity-dispersion profiles, Fuller & Myers (1992; hereafter FM) and Caselli & Myers (1995; hereafter CM) have compiled linewidth measurements in at least three different molecular lines for each of 14 low-mass and 24 massive cores. The resulting σ vs. r profiles indicate that, over similar ranges $r \sim 0.1 - 1$ pc in all the clumps, and independently of whether or not stars are present within them, the velocity dispersion rises more steeply with radius in low-mass cores than in high-mass ones. In particular, nonthermal linewidths in the former are consistent with $\sigma_{\rm NT} \propto r^{0.53}$; in the latter, $\sigma_{\rm NT} \propto r^{0.21}$ (CM). In our view, this situation is a direct result of the effect summarized by equation (4.13). That is, we consider the low-mass cores of FM to be eminently stable logotropes truncated at small ξ, while the high-mass clumps of CM are near critical stability and hence have smaller r_0. The two surveys target similar r within each type of core, so the massive-core data apply to larger dimensionless ξ, and must sample the shallower parts of velocity-dispersion profiles like those in Fig. 2.

To actually confront the predictions of our logotropic equation of state with the observations of FM and CM, we again identify the (model) central velocity dispersion with the (observed) thermal linewidth: $\sigma_c^2 = \sigma_{\rm T}^2 = kT/\mu m_H$, where T is taken from CM, and $\mu = 2.33$. CM assume $T = 10$ K for all the low-mass cores, and we further assume them all to have $P_s \approx P_c$; they should therefore have a common r_0, which may be easily estimated. Five of the FM cores are observed at radii $r_{\rm TNT}$ such that $\sigma_{\rm NT} = \sigma_{\rm T}$; among these, $\langle r_{\rm TNT} \rangle \simeq 0.12$ pc (see Table 3 of CM). The related quantity $\xi_{\rm TNT} = r_{\rm TNT}/r_0$ in a model logotrope is just that point where $\sigma^2/\sigma_c^2 = (\sigma_{\rm NT}^2 + \sigma_{\rm T}^2)/\sigma_{\rm T}^2 = 2$. If, for example, $A = 0.2$ in equation (4.1), we find $\xi_{\rm TNT} = 0.51$, and thus

$$r_0({\rm low}) \approx 0.25 \ {\rm pc} \ .$$

This result is then used in equation (4.13), along with $\sigma_c^2 \propto T$ and $A = 0.2$, to give

$$r_0({\rm high}) \approx 0.056 \ {\rm pc} \ \left(\frac{T_{\rm high}}{10 \ {\rm K}} \right) \ ,$$

where $12 \ {\rm K} \leq T \leq 33$ K for the massive cores (CM). The data may now be appropriately scaled and compared to theoretical $\sigma - r$ and $\sigma_{\rm NT} - r$ curves.

Figure 3 is the result of such a comparison with three logotropes of different A. The good overall agreement between the models and data suggests that GMC cores are well described by

$$A_{\rm core} = 0.20 \pm 0.02 \ ,$$

which is encouragingly close to $A_{\rm GMC}$ as given in equation (4.11) above. In Table 1 we list the radii and other properties (as calculated from eqs. [4.4] to [4.7] above) of critical logotropes with A near 0.2.

Some of the scatter in Fig. 3 could arise if A does not have a common value for all cores, and any embedded stars could further complicate the situation. (Notably, FM and CM both find that starless cores alone show a tighter — but not different — linewidth-radius relation than do cores with stars, suggesting that the basic form seen here is one of the initial conditions for star formation.) However, some of the scatter is surely due to the fact that the cores in this sample do not reside in a single GMC, but come from diverse environments. (For instance, the low-mass cores here tend to be found in dark clouds of mass $\sim 10^4 - 10^5 M_\odot$, and the high-mass ones in somehat larger GMCs.) Thus, there is no guarantee that every low-mass core observes $P_s \approx P_c$, or that every high-mass core is at its critical mass. It is the large number of cores available here which allows the mean trend in Fig. 3, and the implied structural dichotomy between small and large clumps, to emerge.

As with our earlier consideration of core-to-GMC density and linewidth ratios, a fit of similar quality to the data in Fig. 3 can be obtained with the model velocity-dispersion profile of an $n = 2$

polytrope which has a scale r_0 about a factor of two smaller than that used here. As we have stressed, however, there are other difficulties with the application of polytropic equations of state to GMCs and cores.

In summary, the approach we have taken self-consistently allows for purely thermal motions to dominate on the smallest scales in cores (and in GMCs); for an internal density structure ($\rho \propto r^{-1}$ in the outer parts of cores, and much shallower near their centers) which is consistent with at least some observations[1] (Cernicharo et al. 1985; Stüwe 1990; André, Ward-Thompson, & Barsony 1993); and for a unified treatment of low- and high-mass cores. This is in contrast to the models of FM and CM (also Myers & Fuller 1992), which assume two distinct components of isothermal and nonthermal gas in cores and predict a $\rho \propto r^{-2}$ singularity at their centers. It should also be noted that the assumption $P_s \approx P_c$ in low-mass cores still allows for these noncritical clumps to show a fair degree of central concentration. For example, an $A = 0.2$ logotrope which is truncated at $\xi \simeq 0.1\ \xi_{\rm crit}$ has $\rho_s/\rho_c < 0.09$, but $P_s/P_c \simeq 0.5$; thanks to the relatively weak dependence of P on ρ, we do not require, nor even expect, that all low-mass cores be uniform-density spheres. Our model is therefore consistent with the significantly non-uniform density profiles of low-mass cores ($\alpha_{\rm mag} \gtrsim 3$) in the Rosette GMC (Williams et al. 1995).

5. Summary

We have generalized the classic Bonnor-Ebert relations for isothermal spheres, to give expressions for the masses, radii, and total velocity dispersions of magnetized, pressure-truncated gas clouds with any internal pressure-density relation. The analysis combines an exact approach, based on solving the equation of hydrostatic equilibrium, with a virial-theorem treatment to incorporate mean magnetic fields into the clouds. A stability criterion has been developed that relies only on the assumption of an invariant central velocity dispersion σ_c, and is independent of the gas equation of state. Clouds which are just *critically* stable under this condition have mass-radius and size-linewidth relations which are effectively oblivious to their internal structure, i.e., to their equation of state.

These results have been applied to molecular cloud complexes and dense cores, leading to three main conclusions:

---

[1]Williams et al. (1995) fit the projected density profiles of many clumps in the Rosette GMC, with a function of the form $(1 + r_p/a)^{-n}$ — a being the projected half-power radius. They find $n \approx 1$ outside of unresolved central regions, and suggest that this implies an intrinsic density profile of $\rho \propto r^{-2}$. However, because molecular cores have a finite extent, their density profiles in projection are not so simply related to their space densities. (For example, the surface density of a core with *any* ρ profile must decline steeply in the outermost regions, as less and less of the core material is intercepted by the line of sight.) Even a truncated logotrope, for which we might naively expect a flat surface-density profile, actually gives rise to something consistent with $n \approx -0.8$ to -1.0 over most radii in the fitting function of Williams et al.; and the projected half-power radius is only $a = 2.92 r_0 \sim 0.2$ pc for a critical, $A = 0.2$ core ($R_{\rm crit} = 24.37 r_0$).

(1) In spite of their nonspherical geometry, the gross features of GMCs are consistent with those of critical-mass clouds in our analysis. (In the context of GMCs and cores, we identify the central velocity dispersion with the *thermal* part of the total [thermal plus turbulent] linewidth.) *Independently of the exact equation of state*, if equipartition between magnetic and kinetic energies obtains in a critically stable cloud, then it will appear to be in simple gravitational equilibrium, $2\,\mathcal{U}+\mathcal{W}\approx 0$ (equivalently, it will have a virial parameter $\alpha_{\rm mag}\simeq 1$). These are observed features of real GMCs and their most massive cores. In addition, any of our critical-mass spheres obey the same mass-radius and size-linewidth relations which hold among real GMCs. All of this implies that GMCs, and large clumps, are near criticality.

(2) No polytropic (power-law) pressure-density relation can fully characterize GMCs or cores. A positive polytropic index leads to a velocity dispersion which decreases outwards within a cloud, opposite to what is seen both in individual cores and in entire cloud complexes. Alternatively, a negative index (i.e., $P\propto\rho^{\gamma}$ with $\gamma<1$) gives a linewidth which increases with radius, as required. However, such clouds do not show virial parameters near unity unless their mean fields are so strong that their magnetic and gravitational energies are comparable in magnitude, and this is again in conflict with observations of GMCs and large cores. Given our stability criterion, an equivalent statement is that pressure-truncated polytropes are unconditionally stable against gravitational collapse. Since weakly damped Alfvén waves satisfy $P\propto\rho^{1/2}$ (McKee & Zweibel 1995), this shows explicitly that they cannot fully explain the observed nonthermal support in molecular clouds.

(3) The most successful model for the internal structure of molecular cores, and one which is also consistent with global properties of GMCs, is a "pure logotrope:" $P/P_c = 1 + A\,\ln(\rho/\rho_c)$. This relation is meant to account for *all* contributions to the total gas pressure, including the effects of disordered magnetic fields (MHD turbulence). Once it is recognized that low-mass cores are far below their critical masses (though still in virial equilibrium; they are essentially pressure-confined), and that high-mass cores are near criticality, the internal velocity-dispersion profiles of clumps from a variety of environments are seen to be consistent with a logotropic model with $A\simeq 0.2$. A similar value of A can also explain characteristic core-to-GMC ratios of mean densities and linewidths, and any A is consistent with the observed size-linewidth relation between GMCs because the logotropic equation of state allows for critical equilibria. Finally, the equilibrium density profile of a logotrope has $\rho\propto r^{-1}$, outside of a constant-density central region. There is some observational support to be found for this prediction, in GMCs and cores both.

We would like to thank Phil Myers for his comments on an earlier version of this paper, and Charles Curry for valuable discussions. R.E.P. also acknowledges conversations with Paola Caselli and Gary Fuller. This work was supported in part by the Natural Sciences and Engineering Research Council of Canada.

A. PRESSURE-TRUNUCATED EQUILIBRIA

For a spherical cloud in hydrostatic equilibrium, with kinematic (thermal plus turbulent) pressure $P = \rho\sigma^2$ (so that σ is the one-dimensional velocity dispersion) and a self-gravitational potential ϕ, we define

$$\psi = \frac{\phi - \phi_c}{\sigma_c^2}, \qquad r_0^2 = \frac{9\sigma_c^2}{4\pi G\rho_c}, \qquad \text{and} \qquad \xi = r/r_0,$$

where a subscript c denotes evaluation of a quantity at the cloud center. The characteristic scale of a cloud is set by r_0; the factor of 9 in its definition identifies it with the projected half-power radius of an isothermal sphere (e.g., Binney & Tremaine 1987). The equation of hydrostatic equilibrium then reads

$$\frac{d}{d\xi}\left(\frac{P}{P_c}\right) = -\frac{\rho}{\rho_c}\frac{d\psi}{d\xi} \ , \tag{A1}$$

and Poisson's equation becomes

$$\frac{1}{\xi^2}\frac{d}{d\xi}\left(\xi^2\frac{d\psi}{d\xi}\right) = 9\frac{\rho}{\rho_c} \ . \tag{A2}$$

(Note that $\psi = d\psi/d\xi = 0$ at $\xi = 0$, and $\psi > 0$ for $\xi > 0$.) The mass enclosed within radius ξ is given by

$$M \equiv M(\xi) = 4\pi\rho_c r_0^3 \int_0^\xi \xi'^2 \frac{\rho}{\rho_c}\, d\xi' \ ,$$

so that, with the help of equation (A2),

$$M = \frac{4\pi}{9}\rho_c r_0^3 \left(\xi^2\frac{d\psi}{d\xi}\right) = \frac{\sigma_c^2 r_0}{G}\left(\xi^2\frac{d\psi}{d\xi}\right) \ . \tag{A3}$$

Following Ebert (1955) and Bonnor (1956), the surface of the cloud is defined by that radius ξ at which the internal pressure $P(\xi)$ just equals a confining pressure P_s due to a surrounding medium of negligible gravity. Equation (A3), the definition of r_0, and the identity $P_c = \rho_c\sigma_c^2$ then yield, for any equation of state relating P and ρ,

$$M = \sqrt{\frac{9}{4\pi}}\left(\xi^2\frac{d\psi}{d\xi}\right)\left(\frac{P_s}{P_c}\right)^{1/2}\frac{\sigma_c^4}{(G^3P_s)^{1/2}} \ . \tag{A4}$$

The physical radius of the cloud is $R = \xi r_0$:

$$R = \sqrt{\frac{9}{4\pi}}\,\xi\left(\frac{P_s}{P_c}\right)^{1/2}\frac{\sigma_c^2}{(GP_s)^{1/2}} \ . \tag{A5}$$

These relations combine to give

$$\Sigma \equiv \frac{M}{\pi R^2} = \sqrt{\frac{4}{9\pi}}\,\frac{d\psi}{d\xi}\left(\frac{P_s}{P_c}\right)^{-1/2}\left(\frac{P_s}{G}\right)^{1/2} \tag{A6}$$

and

$$\rho_{\rm ave} \equiv \frac{3M}{4\pi R^3} = \frac{1}{3}\left(\frac{1}{\xi}\frac{d\psi}{d\xi}\right)\left(\frac{P_s}{P_c}\right)^{-1}\frac{P_s}{\sigma_c^2} \ . \tag{A7}$$

Given an equation of state, the integration of equations (A1) and (A2) determines $d\psi/d\xi$ and P_s/P_c at any truncation radius ξ. This fixes the coefficients in equations (A4)–(A7) and affords mass-radius and size-linewidth relations for pressure-truncated clouds. (Note that the scalings in these relations — $M \propto \sigma^4/P_s^{1/2}$, $R \propto \sigma^2/P_s^{1/2}$, etc. — are *global* ones, and do not necessarily reflect the radial dependence of any quantity *inside* a cloud.)

The definition of the non-uniformity parameter a (eq. [2.5]) allows it to be found as a function of radius:

$$a = \frac{15}{\xi^3}\left(\frac{d\psi}{d\xi}\right)^{-2}\int_0^{\xi} \xi'^3 \frac{d\psi}{d\xi'}\frac{\rho}{\rho_c}\, d\xi' \ ; \tag{A8}$$

and equation (A3) implies that the virial parameter $5\sigma_{\rm ave}^2 R/GM$ for nonmagnetic clouds (i.e., $\alpha_{\rm mag} = \alpha_{\rm non}$) is just

$$\alpha_{\rm non} = 5\frac{\sigma_{\rm ave}^2}{\sigma_c^2}\left(\xi\frac{d\psi}{d\xi}\right)^{-1} \ , \tag{A9}$$

which tends to be a nonincreasing function of ξ. Alternatively, equations (A7) and (2.8d) give

$$\alpha_{\rm non} - a = 15\left(\frac{d\psi}{d\xi}\right)^{-2}\left(\frac{P_s}{P_c}\right) \ . \tag{A10}$$

These results can be used to rewrite equations (A4)–(A7) in terms of $\alpha_{\rm non}$, a, and $\sigma_{\rm ave}$; equations (2.8) (with $\alpha_{\rm mag} = \alpha_{\rm non}$) are then obtained. Also, once $\alpha_{\rm non}$ is known as a function of radius in any cloud, the observable $\alpha_{\rm mag}$ for a given magnetic field configuration may be calculated (e.g., §2.3).

B. STABILITY CRITERION

We begin by recalling the definition of the scale radius r_0 from equation (A3):

$$r_0 = \frac{GM}{\sigma_c^2}\left(\xi^2\frac{d\psi}{d\xi}\right)^{-1} ; \tag{B1}$$

and rearranging equation (A4):

$$P_s = \frac{9}{4\pi}\left(\xi^2\frac{d\psi}{d\xi}\right)^2\left(\frac{P_s}{P_c}\right)\frac{\sigma_c^8}{G^3M^2} \ . \tag{B2}$$

The stability of a cloud truncated at radius R by the external pressure P_s is determined by the sign of the derivative $(\partial P_s/\partial R)$: this is negative for a stable equilibrium, 0 for the "critical" cloud, and positive for instability.

We now apply a perturbation $R \rightarrow R + dR$, while keeping the mass M and central (i.e., thermal) velocity dispersion σ_c of the cloud fixed, so that

$$\left(\frac{\partial P_s}{\partial R}\right)_{M,\sigma_c} = \left(\frac{\partial P_s}{\partial \xi}\right)_{M,\sigma_c} \left(\frac{\partial \xi}{\partial R}\right)_{M,\sigma_c} . \tag{B3}$$

Then $R = \xi r_0$ and equation (B1) give us

$$\begin{aligned} \left(\frac{\partial \xi}{\partial R}\right)_{M,\sigma_c} &= \frac{1}{r_0}\left[1 + \frac{\xi}{r_0}\left(\frac{\partial r_0}{\partial \xi}\right)_{M,\sigma_c}\right]^{-1} \\ &= \frac{1}{r_0}\left[1 - \xi\left(\xi^2 \frac{d\psi}{d\xi}\right)^{-1} \frac{d}{d\xi}\left(\xi^2 \frac{d\psi}{d\xi}\right)\right]^{-1} \\ &= \frac{1}{r_0}\left[1 - 9\xi\left(\frac{d\psi}{d\xi}\right)^{-1} \frac{\rho_s}{\rho_c}\right]^{-1} , \end{aligned} \tag{B4}$$

where ρ_s is the density just inside the cloud edge and we have used Poisson's equation (A2). We also have, from equation (B2),

$$\begin{aligned} \left(\frac{\partial P_s}{\partial \xi}\right)_{M,\sigma_c} &= P_s \left(\frac{d\psi}{d\xi}\right)^{-1} \left(\frac{P_c}{P_s}\right) \left[\left(2\frac{d^2\psi}{d\xi^2} + \frac{4}{\xi}\frac{d\psi}{d\xi}\right)\left(\frac{P_s}{P_c}\right) + \left(\frac{d\psi}{d\xi}\right)^2 \frac{d}{d\psi}\left(\frac{P_s}{P_c}\right)\right] \\ &= P_s \left(\frac{d\psi}{d\xi}\right)^{-1} \left(\frac{\rho_s}{\rho_c}\right) \left[18 - \left(\frac{d\psi}{d\xi}\right)^2 \left(\frac{P_s}{P_c}\right)^{-1}\right] , \end{aligned} \tag{B5}$$

where both equations (A1) and (A2) have been used.

Thus, equations (B3), (B4), and (B5) show that

$$\left(\frac{\partial P_s}{\partial R}\right)_{M,\sigma_c} = 18\frac{P_s}{R}\left[\frac{1 - (1/18)(d\psi/d\xi)^2(P_s/P_c)^{-1}}{(1/\xi)(d\psi/d\xi)(\rho_c/\rho_s) - 9}\right] . \tag{B6}$$

Now, from equations (A10) and (A7), we have

$$\frac{1}{18}\left(\frac{d\psi}{d\xi}\right)^2 \left(\frac{P_s}{P_c}\right)^{-1} = \frac{5}{6}\frac{1}{\alpha_{\rm non} - a} \qquad \text{and} \qquad \frac{1}{\xi}\left(\frac{d\psi}{d\xi}\right) = 3\frac{\rho_{\rm ave}}{\rho_c} ,$$

so that finally,

$$\left(\frac{\partial P_s}{\partial R}\right)_{M,\sigma_c} = -6\frac{P_s}{R}\left[\frac{1 - (5/6)(\alpha_{\rm non} - a)^{-1}}{3 - \rho_{\rm ave}/\rho_s}\right] . \tag{B7}$$

Alternatively, for a *nonmagnetic* cloud, we can make use of equation (2.8c), with $\alpha_{\rm mag} = \alpha_{\rm non}$, to write

$$\left(\frac{\partial P_s}{\partial R}\right)_{M,\sigma_c} = -6\frac{P_s}{R}\left[\frac{1 - (\pi G \Sigma^2)/(8P_s)}{3 - \rho_{\rm ave}/\rho_s}\right] . \tag{B8}$$

This treatment is valid for *any* gas equation of state, so long as the cloud radius is perturbed in such a way that M and σ_c are unaffected. The result (B8) was also obtained by Ebert (1955) and

Bonnor (1956), who specifically considered the stability of truncated isothermal spheres, and by Maloney (1988) in his study of negative-index polytropes.

Any virialized cloud truncated at small ξ (i.e., where ρ and σ^2 are approximately constant) will be stable. This is because, regardless of the equation of state, the potential ψ at small radii can always be expanded in a power series of the form: $\psi = (3/2)\xi^2 - \mathcal{O}(\xi^4)$ (see Appendix C for an example). Thus, referring to equation (B6) with $\rho_s \approx \rho_c$, we have $(\partial P_s/\partial R)_{M,\sigma_c} \approx -3P_s/R < 0$. Depending on the equation of state, there may or may not be a truncation at larger ξ which results in $(\partial P_s/\partial R)_{M,\sigma_c} > 0$ and an unstable equilibrium.

C. POLYTROPES OF NEGATIVE INDEX

Consider the (nonmagnetic) equation of state

$$P \propto \rho^{1+1/N},$$

where the polytropic index $N < -1$. Then we define $n = N/(N+1)$ and write

$$P = \rho_c \sigma_c^2 \left(\frac{\rho}{\rho_c}\right)^{1/n}, \qquad n \geq 1, \tag{C1}$$

with $n = 1$ corresponding to isothermality. In order to evaluate the coefficients in equations (A4)–(A7) (or [2.8], with $\alpha_{\rm mag} = \alpha_{\rm non}$), we first use the relation (C1) to integrate the equation of hydrostatic equilibrium (A1) and find

$$\frac{\rho}{\rho_c} = [1 + (n-1)\psi]^{n/(1-n)}, \tag{C2}$$

so that Poisson's equation (A2) becomes

$$\frac{1}{\xi^2}\frac{d}{d\xi}\left(\xi^2 \frac{d\psi}{d\xi}\right) = 9[1 + (n-1)\psi]^{n/(1-n)}. \tag{C3}$$

(Note that in the limit $n \to 1$, the right-hand side of eq. [C3] becomes $9e^{-\psi}$, just what is required for the isothermal sphere.) At the cloud center, $\psi = d\psi/d\xi = 0$, so for small ξ the potential ψ can be expanded in a power series,

$$\psi \longrightarrow \frac{3}{2}\xi^2 - \frac{3n}{40}\xi^4 + \mathcal{O}(\xi^6), \tag{C4}$$

allowing for an integration of equation (C3). The result of this is a core-halo structure to the cloud: at very small radii, the solution is indistinguishable from that for an isothermal sphere, and the density and velocity dispersion are essentially constant with ξ, independently of n. Once $\xi \gtrsim$ a few, however, a power-law density profile obtains; for each n, there exists a singular solution to which the equilibrium cloud tends at large radii.

These singular solutions are readily found by substituting the prescription

$$\frac{\rho}{\rho_c} = K\xi^{-p}$$

into equation (C2) and solving (C3) for K and p. This gives

$$p = \frac{2n}{2n-1} \qquad \text{and} \qquad K = \left[\frac{2}{9}\,(p-1)(3-p)\right]^{p/2}, \tag{C5}$$

so that with $n \geq 1$ we have $1 < p \leq 2$, and these clouds are diffuse enough that they have no "natural" edge. That is, the density never vanishes, and any boundary to the cloud must be defined by the point at which the internal pressure matches that of an external medium. (It is again worth noting the exact correspondence to the singular isothermal sphere when $n = 1$ in eq. [C5]; cf. Chandrasekhar 1967.)

Consider now a polytrope of negative index, which is truncated at radius ξ large enough that the structure of the cloud is given by the singular solution. Then $d\psi/d\xi$ and P_s/P_c can be calculated analytically, and equation (A10) yields

$$\alpha_{\rm non} - a = \frac{5}{6}(4n-3)\ . \tag{C6}$$

We also know that $a = (1 - p/3)/(1 - 2p/5)$, so

$$\alpha_{\rm non} = \frac{5}{2}\ \frac{(4n-3)(2n-1)}{6n-5} \tag{C7}$$

and we have the following:

$$M = \sqrt{\frac{2}{\pi(4n-3)^3}}\ \left(\frac{6n-5}{2n-1}\right)^2\ \frac{\sigma_{\rm ave}^4}{(G^3P_s)^{1/2}}\ , \tag{C8}$$

$$R = \sqrt{\frac{1}{2\pi(4n-3)}}\ \frac{6n-5}{2n-1}\ \frac{\sigma_{\rm ave}^2}{(GP_s)^{1/2}}\ , \tag{C9}$$

$$\Sigma = \sqrt{\frac{8}{\pi(4n-3)}}\ \left(\frac{P_s}{G}\right)^{1/2}\ , \tag{C10}$$

and

$$\rho_{\rm ave} = \frac{6n-3}{6n-5}\ \frac{P_s}{\sigma_{\rm ave}^2}\ . \tag{C11}$$

Thus, regardless of where they are truncated by the surface pressure P_s, these model clouds can only ever represent modest enhancements over the intercloud medium. In particular, $P_{\rm ave}/P_s$ has a maximum of 3 (for isothermality, $n = 1$), but even for $n = 2$ (which gives the ρ dependence of Alfvén wave pressure; McKee & Zweibel 1995) is reduced to just 9/7.

As discussed in §3, any truncation of a negative-index polytrope results in a stable cloud. This is because, with $\rho \propto r^{-p}$, we have that $\rho_{\rm ave}/\rho_s = 3/(3-p)$, and the stability criterion (B7) becomes (with the help of [C6]) $(\partial P_s/\partial R)_{M,\sigma_c} = -4P_s/R < 0$. In particular, this holds in the limit $n \to 1$, when the numerator and denominator of (B7) both vanish. What allows for the existence of critical and unstable equilibria for the bounded isothermal sphere, then, is the fact that its density profile actually oscillates about the singular solution $\rho \propto r^{-2}$ at large radii (Chandrasekhar 1967). This does *not* occur for those polytropes with $n > 1$; instead, the bounded spheres follow the singular solutions exactly at large ξ.

Finally, it is worth noting that these results do not contradict the well known instability (e.g., Shu 1977) of truly singular spheres, for which $\rho \propto r^{-p}$ all the way to the center and $\rho_c \to \infty$. In such cases, perturbation of the truncated cloud radius is performed with M, σ_c, *and* ρ_c all held fixed. Stability then depends only on the sign of $(\partial P_s/\partial \xi)_{M,\sigma_c}$ (eq. [B5]), which is always positive for these polytropes.

Table 1. Properties of Critical Logotropes.

A	$\xi_{\rm max}$	$\xi_{\rm crit}$	ρ_s/ρ_c	σ_s^2/σ_c^2	$\sigma_{{\rm NT},s}^2/\sigma_c^2$	P_s/P_c
0.18	51.73	40.29	4.96×10^{-3}	9.07	8.07	0.045
0.20	31.29	24.37	8.65×10^{-3}	5.78	4.78	0.050
0.22	20.83	16.22	1.36×10^{-2}	4.04	3.04	0.055

REFERENCES

André, P., Ward-Thompson, D., & Barsony, M. 1993, ApJ, 406, 122

Arons, J., & Max, C. E. 1975, ApJ, 196, L77

Binney, J., & Tremaine, S. 1987, Galactic Dynamics (Princeton: Princeton Univ. Press)

Bertoldi, F., & McKee, C. F. 1992, ApJ, 395, 140

Bonnor, W. B. 1956, MNRAS, 116, 351

Carr, J. S. 1987, ApJ, 323, 170

Caselli, P., & Myers, P. C. 1995, ApJ, 446, 665 (CM)

Cernicharo, J., Bachiller, R., & Duvert, G. 1985, A&A, 149, 273

Chandrasekhar, S. 1967, An Introduction to the Study of Stellar Structure (New York: Dover)

Chièze, J. P. 1987, A&A, 171, 225

de Jong, T., Dalgarno, A., & Boland, W. 1980, A&A 91, 68

Ebert, R. 1955, ZAp, 37, 217

Elmegreen, B. G. 1985, in Protostars & Planets II, ed. D. Black & M. Matthews (Tucson: Univ. of Arizona Press), p. 33

Elmegreen, B. G. 1989, ApJ, 338, 178

Falgarone, E., Phillips, T. G., & Walker, C. K. 1991, ApJ, 378, 186

Fleck, R. C., Jr. 1988, ApJ, 328, 299

Fuller, G. A., & Myers, P. C. 1992, ApJ, 384, 523 (FM)

Gehman, C. S., Adams, F. C., Fatuzzo, M., & Watkins, R. 1996, ApJ, 457, 718

Harris, W. E., & Pudritz, R. E. 1994, ApJ, 429, 177

Heiles, C., Goodman, A., McKee, C. F., & Zweibel, E. G. 1993, in Protostars and Planets III, ed. E. H. Levy & J. I. Lunine (Tucson: Univ. of Arizona Press), p. 279

Henriksen, R. N. 1991, ApJ, 377, 500

Lada, E. A., Bally, J., & Stark, A. A. 1991, ApJ, 368, 432

Larson, R. B. 1981, MNRAS, 194, 809

Lizano, S., & Shu, F. H. 1989, ApJ, 342, 834

Loren, R. B. 1989, ApJ, 338, 925

Maloney, P. 1988, ApJ, 334, 761

McCrea, W. H. 1957, MNRAS, 117, 562

McKee, C. F. 1989, ApJ, 345, 782

McKee, C. F., & Zweibel, E. G. 1992, ApJ, 399, 551

McKee, C. F., & Zweibel, E. G. 1995, ApJ, 440, 686

Miesch, M. S., & Bally, J. 1994, ApJ, 429, 645

Mouschovias, T. Ch. 1987, in Physical processes in Interstellar Clouds, ed. G. E. Morfill & M. Scholer (Dordrecht: Reidel), p. 453

Mouschovias, T. Ch., & Psaltis, D. 1995, ApJ, 444, L105

Mouschovias, T. Ch., & Spitzer, L. 1976, ApJ, 210, 326

Myers, P. C., & Fuller, G. A. 1992, ApJ, 396, 631

Myers, P. C., & Goodman, A. A. 1988a, ApJ, 326, L27

Myers, P. C., & Goodman, A. A. 1988b, ApJ, 329, 392

Myers, P. C., Fuller, G. A., Goodman, A. A., & Benson, P. J. 1991, ApJ, 376, 561

Nakano, T. 1984, Fund. Cosmic Phys., 9, 139

Pudritz, R. E. 1990, ApJ, 350, 195

Sanders, D. B., Scoville, N. Z., & Solomon, P. M. 1985, ApJ, 289, 373

Scoville, N. Z., Yun, M. S., Clemens, D. P., Sanders, D. B., & Waller, W. H. 1987, ApJS, 63, 821

Shu, F. H. 1977, ApJ, 214, 488

Shu, F. H., Milione, V., Gebel, W., Yuan, C., Goldsmith, D. W., & Roberts, W. W. 1972, ApJ, 173, 557

Solomon, P. M., Rivolo, A. R., Barrett, J., & Yahil, A. 1987, ApJ, 319, 730

Stutzki, J., & Güsten, R. 1990, ApJ, 356, 513

Stüwe, J. A. 1990, A&A, 237, 178

Tomisaka, K., Ikeuchi, S., & Nakamura, T. 1988, ApJ, 335, 239

Viala, Y. P., & Horedt, G. P. 1974, A&A, 33, 195

Waller, W. H., Clemens, D. P., Sanders, D. B., & Scoville, N. 1987, ApJ, 314, 397

Williams, J. P., Blitz, L., & Stark, A. A. 1995, ApJ, 451, 252

Williams, J. P., de Geus, E. J., & Blitz, L. 1994, ApJ, 428, 693

This preprint was prepared with the AAS LaTeX macros v4.0.

Fig. 1.— Comparison of the logotropic equation of state $[P/P_c = 1 + 0.18\ \ln(\rho/\rho_c)]$ with those for Alfvén wave pressure $[P/P_c = (\rho/\rho_c)^{1/2}]$ and a logotrope-plus-isothermal sphere combination $[P/P_c = \rho/\rho_c + 0.1\ \ln(\rho/\rho_c)]$.

Fig. 2.— Structure of a logotropic gas sphere with $A = 0.18$. The vertical line in all four panels is at the truncation radius which makes for a critically stable cloud: $\xi_{\rm crit} = 40.29$. The long-dashed line in the plot of ρ vs. r is the singular density profile of eq. (4.3); that in the plot of total linewidth (bottom left) represents $\sigma^2 \propto r^{2/3}$; and those in the plot of nonthermal linewidth (bottom right) trace $\sigma^2_{\rm NT} \propto r$ and $\sigma^2_{NT} \propto r^{1/2}$. Recall that $r_0^2 \equiv 9\sigma_c^2/4\pi G\rho_c$.

Fig. 3.— Comparison of observed internal velocity-dispersion profiles (total σ, thermal and nonthermal components $\sigma_{\rm T}$ and $\sigma_{\rm NT}$) with logotropic models, for 38 GMC cores. Open squares correspond to low-mass cores (Fuller & Myers 1992), and filled symbols to high-mass cores (Caselli & Myers 1995; we omit four HCO^+ measurements). Cores both with and without stars are represented here, and each has been observed in three or more different molecular lines. The model curves are for $A = 0.20$ (best case; solid line), and $A = 0.18$, $A = 0.22$ (dashed lines); a larger A results in smaller maximum and critical radii r/r_0. The vertical line is at $\xi_{\rm crit} = 24.37$ for an $A = 0.2$ logotrope.

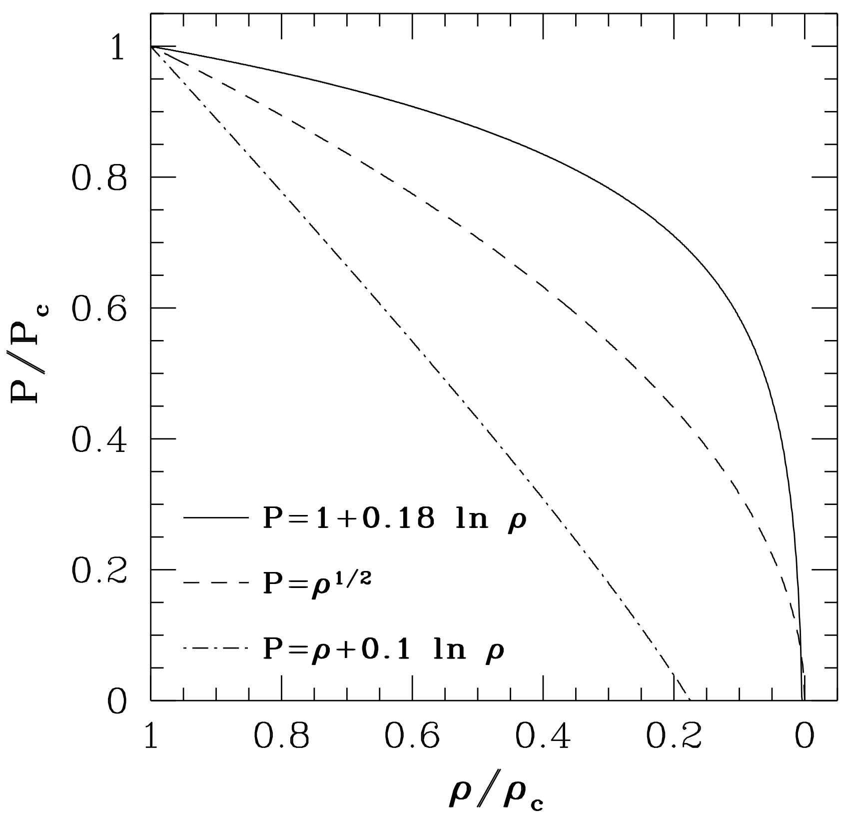
P/P_c
1
0.8
0.6
0.4
0.2
0
P=1+0.18 ln ρ
P=ρ^1/2
P=ρ+0.1 ln ρ
1
0.8
0.6
0.4
0.2
0
ρ/ρ_c

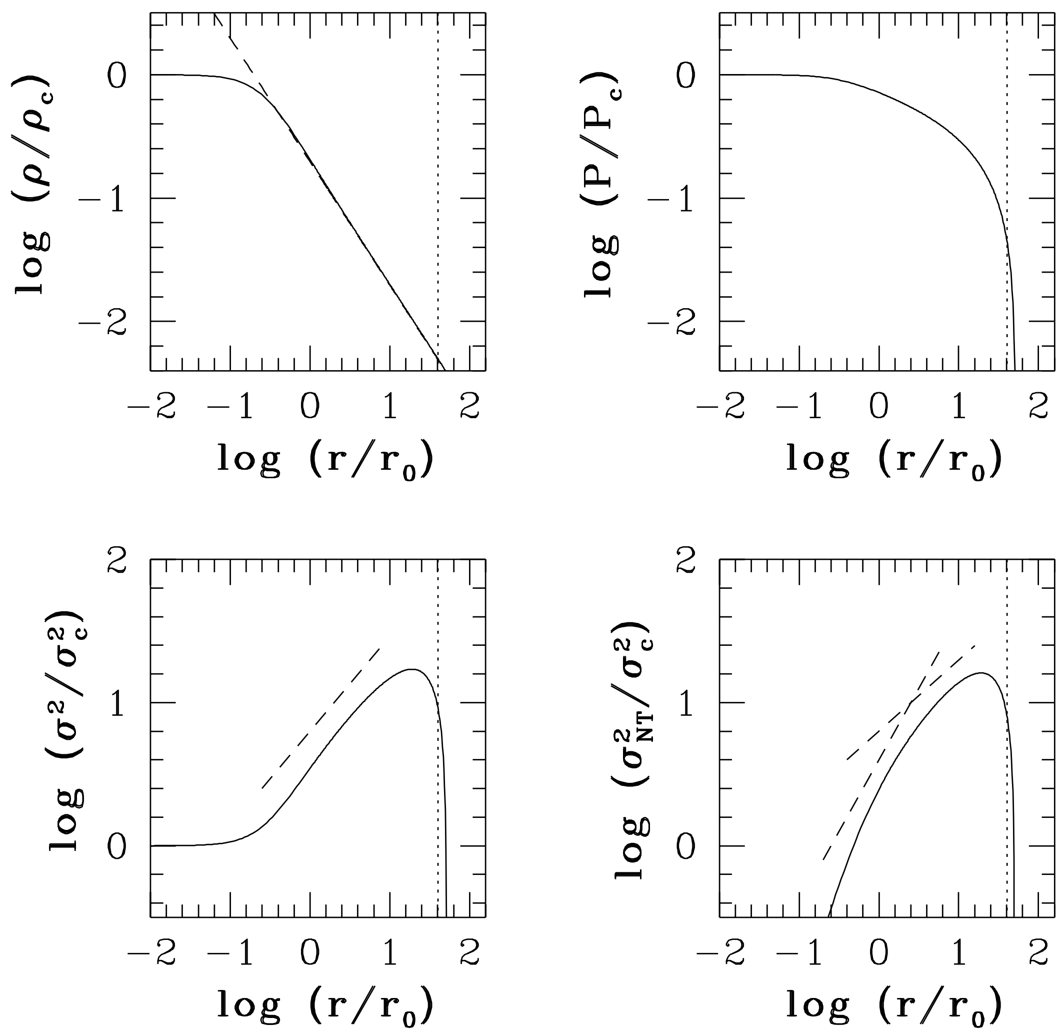
log (ρ/ρ$_c$)
0
−1
−2
−2 −1 0 1 2
log (r/r$_0$)
log (P/P$_c$)
0
−1
−2
−2 −1 0 1 2
log (r/r$_0$)
log (σ^2/σ$_c^2$)
2
1
0
−2 −1 0 1 2
log (r/r$_0$)
log (σ$_{NT}^2$/σ$_c^2$)
2
1
0
−2 −1 0 1 2
log (r/r$_0$)

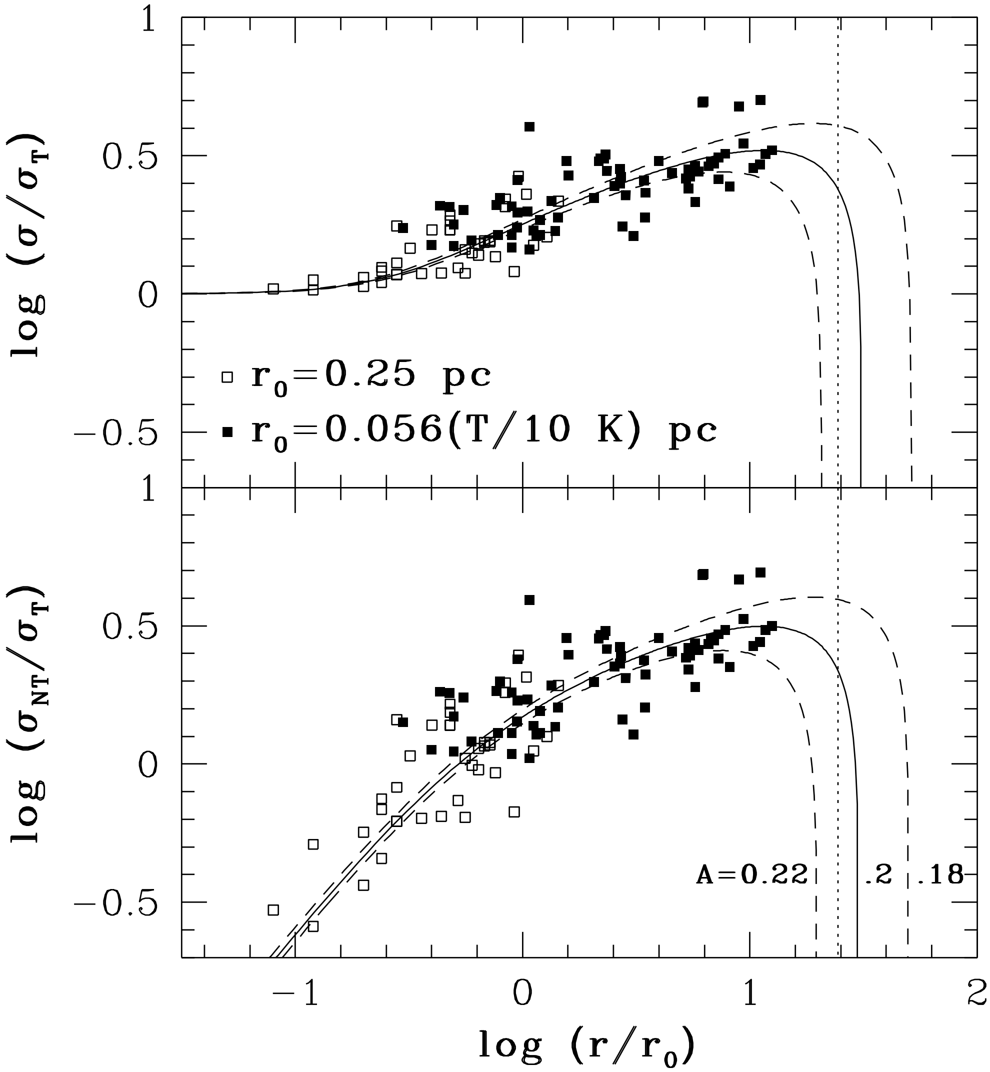
1
0.5
0
−0.5
log (σ/σ_T)
r_0=0.25 pc
r_0=0.056(T/10 K) pc
1
0.5
0
−0.5
log (σ_NT/σ_T)
A=0.22
.2
.18
−1
0
1
2
log (r/r_0)